THE JOURNAL OF PHYSICAL CHEMISTRY C
A JOURNAL OF THE AMERICAN CHEMICAL SOCIETY

pubs.acs.org/JPCC

Article

Ligand-Engineered Spin Crossover in Fe(II)-Based Molecular and Metal−Organic Framework Systems

Published as part of The Journal of Physical Chemistry virtual special issue "Early-Career and Emerging Researchers in Physical Chemistry Volume 2".

Monique C. Demuth,[†] Khoa N. Le,[†] Matthew Sciprint, and Christopher H. Hendon*

Cite This: https://doi.org/10.1021/acs.jpcc.2c08816

Read Online

ACCESS | Metrics & More | Article Recommendations | Supporting Information

ABSTRACT: Some transition metals have valence electrons that can form either high- or low-spin complexes depending on their ligand field. The interconversion between high-to-low or low-to-high spin can also be achieved by changing the temperature, promoting a spin crossover (SCO) event. Such transitions are potentially useful for quantum data storage, catalysis, and beyond. Here we examine the spin-crossover properties of $Fe(ta)_2$ (iron triazolate), a Fe^{2+}-containing metal−organic framework (MOF) that is known to undergo spin crossover. We compare the electronic and geometric properties of the MOF to a related molecular system, monitoring electronic properties before, during, and after the spin transitions. Our data reveals that long-range cooperativity affects the energetics of spin crossover in the MOF, but not the molecule. We attribute these differences to electronic dissimilarities in the ligands and structural differences in the crystal connectivity, and offer design strategies to control SCO in framework materials.

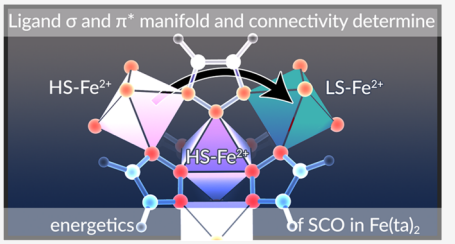

INTRODUCTION

Spin-crossover is an inorganic phenomenon where changes in the local coordination environment result in reordering of the metal valence electrons.[1,2] Although SCO can be promoted with electric fields and light, the transition is often thermally accessed to affect the metal−ligand bond lengths. Since elevated temperatures tend to elongate bonds, high temperatures generally favor high-spin configurations (i.e., weaker ligand fields). This effect is potentially useful in quantum information storage,[3] particularly in the case of octahedral Fe(II) systems,[4] where a geometric metal−ligand bond perturbation is accompanied by transitions between two dissimilar spin configurations. The challenge, however, is designing a chemical system in which the ligand is neither bound too loosely or tightly such that the Fe is able to interconvert between the two spin-states, with controllable hysteresis, i.e., "memory".[5]

This topic has been extensively studied for molecular systems, and some general design principles have been developed.[6] One such principle is the use of N-donor atoms for Fe(II) metal centers, such that a tension is created between Fe(II)'s propensity to form low-spin complexes, further stabilized by N-based donors (moderately strong ligand fields).[7,8] Together, temperature is thought to promote a low-to-high spin transition, resulting in several quantum-chemical measurables. Hysteresis is then a useful tunable property which allows for the spin-state to persist after the stimulus has been removed (e.g., upon cooling the material below the critical temperature).[9,10] One avenue to affect hysteresis is through "cooperativity", where the potential energy barrier for the transition is affected by the energy of a neighboring spin center, in essence accessing a metastable state.

Together these phenomena have seen a renaissance due to the advent of MOFs.[11−14] There, a molecular design approach has been used to develop scaffolds with well-defined metal-coordination environments, while also featuring long-range connectivity.[15] SCO MOFs, however, present some degree of intrigue because the structural perturbation at the metal−ligand interface should affect the bulk MOF because the metal centers are connected to one another, even if they are not in direct electronic communication (magnetically or otherwise).[16−18] Together, there remain several fundamental curiosities related to d-electron ordering in MOFs and how they are impacted by neighboring clusters undergoing spin-transitions.

In previous studies, the metal−organic interface in iron triazolate ($Fe(ta)_2$, Figure 1a) was shown to be dynamic, and a cooperative SCO effect was observed.[19−22] Notably, the SCO

Received: December 16, 2022
Revised: January 11, 2023

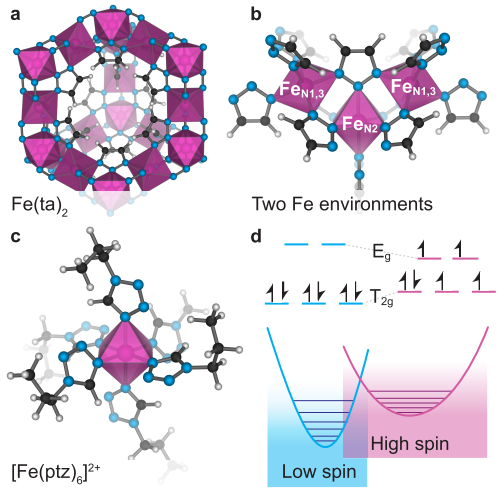

Figure 1. Examination of the metal−ligand environments in the MOF, $Fe(ta)_2$, and molecular solid, $[Fe(ptz)_6](BF_4)_2$. (a) The $Fe(ta)_2$ MOF structure contains two distinct metal environments (b) where either Fe is bound to N2 or N1,3 coordination sites on the 1,2,3-triazolate linker. (c) A single Fe(II) center coordinated to six 1-propyltetrazole linkers at the N4 site from the molecular solid $[Fe(ptz)_6](BF_4)_2$. (d) A schematic depicting a spin-crossover event originating from intersecting low- and high-spin surfaces.

transition is not a redox event, but rather a conversion between low- and high-spin Fe(II). Since there are two dissimilar Fe(II) centers housed within the $Fe(ta)_2$ framework (Figure 1b, four $Fe(II)_{N1,3\text{-connected}}$ and two $Fe(II)_{N2\text{-connected}}$ per computational unit cell), SCO may inherently break symmetry,[23−25] and we surmised that there may be "special" concentrations of $HS(Fe^{2+})$ that may be preferentially stabilized throughout the SCO transition; i.e., one Fe environment may transition preferentially over the other. Alternatively, there may be a temperature-dependent "Devil's staircase" throughout the SCO event;[26] however, the steplike magnetization response to temperature has not been observed in $Fe(ta)_2$.

Beyond crystallography, there is evidence to suggest the Fe-centers in $Fe(ta)_2$ are chemically dissimilar. In one study, oxidation of $Fe(ta)_2$ was shown to yield an electrically conductive material.[27] and prior calculations showed that the installation of a single Fe(III) high-spin center preferentially localized on the N1,3-coordination site, Figure 1b.[28] Although not directly related to SCO, the observation of elevated conductivity indicates a degree of hole delocalization,[29] suggesting that the framework derives its properties from interactions that reach beyond a single Fe−N coordination sphere.

In this paper, we further study the SCO effect by comparing the electronic properties of $Fe(ta)_2$ and a related molecular complex known to also feature a thermally induced SCO transition, $[Fe(ptz)_6](BF_4)_2$ (ptz = 1-propyltetrazole, **Fe-ptz**, Figure 1c).[30] Our rationale is that a molecular analog should allow us to isolate the cooperative effect found in the MOF, while also probing the potential energy surface of the MOF as it undergoes sequential SCO transitions. On the other hand, the molecular crystal features dissimilar ligands (tetrazoles, not triazoles) and no long-range connectivity and will prove to be a useful comparison on both fronts.

COMPUTATIONAL METHODS

Crystallographic structures of $Fe(ta)_2$ and $[Fe(ptz)_6](BF_4)_2$ were obtained from the literature.[27,30] Geometric and electronic relaxations were performed on both structures with an enforced spin of 0 on all Fe atoms (i.e., low spin Fe(II)). The ionic convergence criterion was set to 0.005 eV $Å^{-1}$, and the electronic convergence criterion was set to be 10^{-6} eV. The projected augmented wave (PAW) basis set was used and the plane wave cutoff was set to be 500 eV.[31] All optimizations were performed using periodic boundary conditions within the Vienna *ab initio* Simulation Package (VASP, version 5.4.4.).[32] The PBEsol[33] exchange-correlation functional was first used to obtain the structural minima and was used as the input geometry for our hybrid range-separated functional calculations. HSEsol06 (HSEsol) was then employed for both structure and electronic properties.[34,35] Here, HSEsol06 is differs from conventional HSE06 only by using PBEsol as the base GGA functional, and we include the 06 suffix to delineate between it and a similar functional based on HSE03. Both were fully equilibrated using a gamma-only K-grid.

Octahedral HS Fe^{2+} has 4 unpaired electrons. Both the $Fe(ta)_2$ and **Fe-ptz** unit cells contain 6 Fe-centers. In both cases, each of the LS-optimized unit cells (i.e., $S = 0$, diamagnetic) were then used for structure relaxations with an enforced number of unpaired electrons equal to 0, 4, 8, 12, 16, 20, and 24 in a ferromagnetic configuration, corresponding to an increased number of high spin iron from 0 to 6 in the unit cell of both the molecular crystal and MOF. Both ferro- and antiferromagnetic orientations were sampled, and ferromagnetic orientations were found to be the most stable. Each structure was allowed to fully equilibrate using the same approach used for the low-spin system.

Molecular calculations (e.g., those in Figure 2) were computed in Gaussian09.[36] The structures were obtained by extracting them from their respective LS/HS optimized structures from VASP, then performing a single point calculation using the hybrid exchange-correlation functional HSE06 to determine electrostatic potential and Mulliken charges. A 6-311++G** basis set was chosen as it includes polarization and diffuse functions on all atoms, and should capture subtle changes in electron density at the N-centers.[37]

RESULTS AND DISCUSSION

Both $Fe(ta)_2$ and **Fe-ptz** feature a common octahedral Fe(II) coordination environment, with the latter forming bonds to 1-propyltetrazole linkers, Figure 1c. Unlike $Fe(ta)_2$, **Fe-ptz** is experimentally known to prefer the HS configuration, with LS accessed through controlled quenching. Although both Fe(II) centers are formally 6-coordinate with N-donor, the structures differ in ligand identity and metal-linker bond length. The average computed Fe−N bond lengths in $Fe(ta)_2$ are 1.91 Å (low spin), whereas **Fe-ptz** features an Fe−N length approximately 0.02 Å longer in the ground state (high spin). This subtle difference can be understood from examination of the ground-state electronic structure of the ligand.

Molecular calculations of the electron density colored using the Mulliken charge distribution reveal differences in N-donor atom electron density, Figure 2. First, the triazolate ligand 1,3N atoms have elevated electron density (−0.210 $e^-/Å^3$) compared to 2N (−0.120 $e^-/Å^3$) which aligns with the previous observation that Fe(II) centers in the 2N site are

https://doi.org/10.1021/acs.jpcc.2c08816
J. Phys. Chem. C XXXX, XXX, XXX−XXX

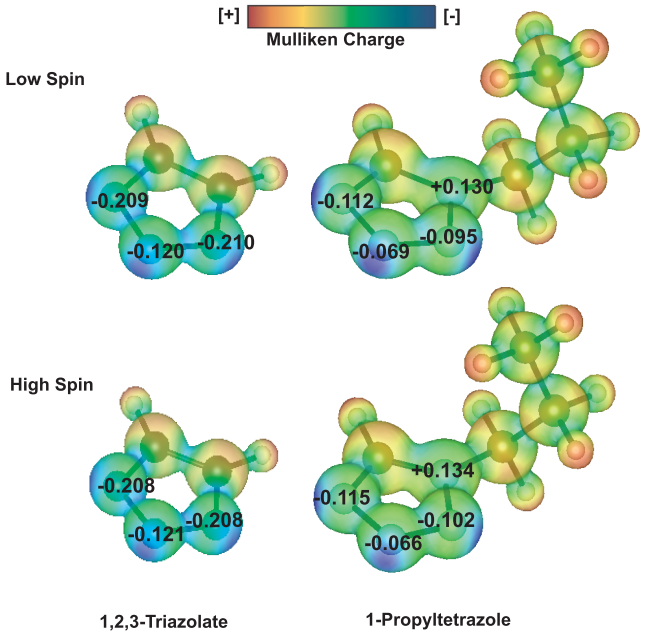

Figure 2. Mulliken charge density projected onto the electron density isosurface of 1,2,3-triazole and 1-propyltetrazole linkers found in $Fe(ta)_2$ and $[Fe(ptz)_6](BF_4)_2$, respectively. The low and high spin linker geometries were obtained from the calculated periodic structures where all Fe centers were spin-paired (LS) and HS, respectively. Single-point DFT calculations were performed to generate Mulliken charges. Values are presented in $e^-/Å^3$.

preferentially oxidized as their d-splitting is reduced.[23] Further, the elevated density on the triazolate linkers indicates the linker should be a stronger field ligand. Conversely, the tetrazole binds through the N4 nitrogen (-0.102 $e^-/Å^3$) indicating it is a much weaker field ligand, despite its similar bond lengths to $Fe(ta)_2$. This important difference leads to markedly different chemical properties between the MOF and molecule. Since e_g orbitals in octahedral systems are affected by the energy of the σ-system, the tetrazole should result in substantially lower e_g orbitals favoring HS complexes in the ground state.

We can model the SCO event by subsequent elongation of the metal−ligand bonds, followed by relaxation of the other bonds and angles in the system. One approach is to create a cluster model of a single Fe-center per the procedure in ref 15. This approach is trivial for the molecular crystal, **Fe-ptz**, but problematic for $Fe(ta)_2$ because it omits long-range interactions. See the Supporting Information for further details. Instead, we performed hydrostatic expansion of the Fe−N bonds in both the bulk MOF, $Fe(ta)_2$, and **Fe-ptz** crystal structure. One can imagine that subsequent spin-transitions do not occur instantaneously, as they rely on significant restructuring of nuclei local to the metal center in both the bulk MOF and the crystallographically ordered molecular solid. Indeed, experimental magnetic measurements show the transition occurs over a narrow temperature range. With this in mind, we sought to gain insight into the nature of cooperativity, i.e., whether one spin-crossover event at one Fe-site affects the energetics of the subsequent events in neighboring sites.

Since both cells contain six Fe centers, we can readily monitor changes in energy as a function of number of HS centers in the cell (installed by forcing a total number of unpaired spins per cell and letting the computation select their localization). In the molecular crystal, the **ptz** ligands are monotopic. We hypothesized that the molecular crystal should not show dramatic increases in lattice parameter nor fluctuate in total energy. Indeed this is the case, as evidenced by both the change in energy and lattice parameters shown in red in Figure 3a,b. Each subsequent LS-to-HS transition only

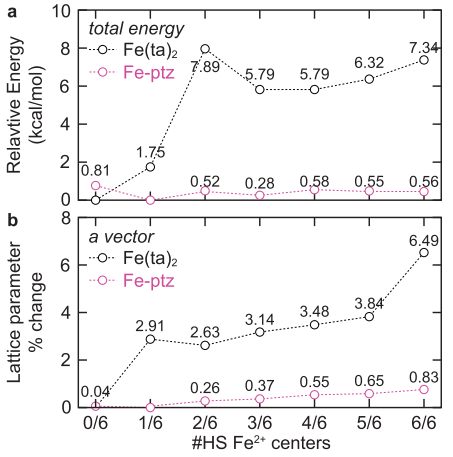

Figure 3. (a) Monitoring the change in total cell energy of $Fe(ta)_2$ and **Fe-ptz** with increasing number of spin-polarized-Fe^{2+}. (b) Percent change of *a* lattice parameters of $Fe(ta)_2$ and **Fe-ptz** with an increasing number of HS-Fe^{2+}. We note that the energy computed for two Fe centers in $Fe(ta)_2$ corresponds to an intermediate spin configuration, Table S2, where one Fe^{2+} is $S = 2$ and two other centers are $S = 1$.

perturbed the system by <1 kcal/mol. Evidently, changes in local Fe−N bond lengths may be accommodated by torsions and reordering of the **ptz** ligand, rather than pushing outward toward other metal centers, but this effect should also be small.

In contrast, $Fe(ta)_2$ shows significantly greater change in energy as more Fe centers become HS. While we needn't worry about the order in which Fe-centers transition in **Fe-ptz**, the MOF poses a more complex problem as the centers interact with one another. To properly assess the lowest energy path for complete SCO, we sampled a variety of spin configurations, shown in Tables S2 and S3. Our exhaustive sampling of the spin configurations revealed an interesting trend. The installation of a single HS center only destabilizes the crystal by 1.8 kcal/mol and localizes on an N1,3 center. But upon addition of two HS centers the crystal is destabilized by 7.9 kcal/mol and delocalizes the second spin across both N2 adjacent Fe-centers. Subsequent spin transitions are lower in energy than the second, indicating that the barrier to SCO is achieved at a critical spin population of 2 Fe per 6 Fe in the cell, or 33%.

However, the structural perturbation did not show the same trend. Figure 3b shows that the lattice parameters of **Fe-ptz** are barely affected by increasing HS centers, whereas the MOF shows an *a*-parameter shift from 11.6 to 12.3 Å, or a total volume expansion of 18% upon SCO (see the Supporting Information for structure files). This supports the prediction that the connectivity of the MOF impacts the energy of each spin transition event.

To further understand the cooperative effects shown in Figure 3 we examined the average Fe−N bond length change as we increase the number of HS Fe^{2+} sites in $Fe(ta)_2$ and **Fe-**

https://doi.org/10.1021/acs.jpcc.2c08816
J. Phys. Chem. C XXXX, XXX, XXX−XXX

ptz (Figure 4). For those sites that underwent a LS-to-HS transition, the change in Fe−N bond length is relatively

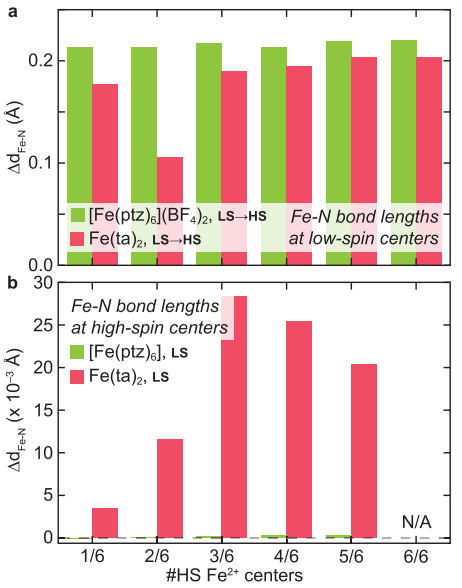

Figure 4. Low-to-high spin transitions come with an accompanying increase in Fe−N bond length (increasing by approximately 0.2 Å). One can monitor the bond lengths of both (a) the Fe centers that have become HS and (b) those that remain LS. One indication of cooperativity is shown in (b), where LS centers in **Fe-ptz** show no geometric dependence to increasing concentration of HS-centers. On the other hand, $Fe(ta)_2$ shows that LS-Fe(II) centers do experience the impact of neighboring HS-Fe(II) within the crystal, evidenced by Fe−N bond elongation at LS-Fe sites.

constant for both $Fe(ta)_2$ and **Fe-ptz** (Figure 4a). The depression observed for 2HS centers is due to the delocalization of the second HS center (see Table S2). For Fe(II) HS centers with localized spin, the Fe−N bond length changes are basically the same as **Fe-ptz**.

We can also monitor the Fe−N bond lengths for sites that have not yet undergone the transition, i.e., LS-Fe(II) in a crystal with some HS sites. For **Fe-ptz**, subsequent SCO events do not affect the bonding of remaining LS-Fe^{2+} centers as evidenced by essentially zero fluctuation in Fe−N bond lengths remote to the HS center (Figure 4b). In the case of $Fe(ta)_2$, the remaining LS-Fe^{2+} sites are affected by their neighboring HS. As a result, a maximum structural perturbation is reached when the MOF has 50% of the sites transition from LS-to-HS, Thus, considering the data in Figures 3 and 4, it appears that the MOF will reach a critical concentration approximately 33−50% structurally perturbed sites before the material will then undergo a structural and spin transition to the HS configuration. From a cooperativity perspective, the energetic peak in potential energy surface (Figure 3a) may be responsible for hysteresis in SCO because a critical population of Fe centers must be geometrically affected before the framework undergoes a transition.

Finally, because Fe^{2+}−SCO results in d-electron restructuring, there should be an accompanied change in electronic band gap. In **Fe-ptz** we expect a reduction in band gap upon LS-to-HS transition, but we would not expect the gap to depend on the number of HS centers, since they are all independent of one another. Our computations support this hypothesis, Figure S4. However, for $Fe(ta)_2$ the Fe centers are affected by the population of HS-Fe^{2+}, and the electronic structure should therefore depend on the number of HS centers. To demonstrate this, we present the all LS, 1HS/5LS, and all HS electronic density of states in Figure 5. A reduction in

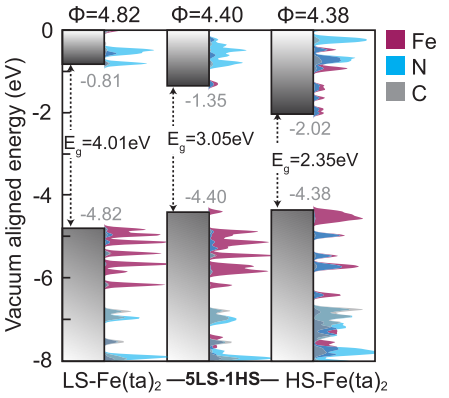

Figure 5. Electronic density of states for $Fe(ta)_2$ as the number of HS-Fe^{2+} sites increase in the unit cell.

electronic gap is observed with increasing HS-Fe^{2+}, but the valence band energy remains unchanged after the installation of a single HS center. This indicates that the electron affinity is affected, which is directly related to the extent of stabilization of the Fe-d orbitals. As a result, spectroscopic measurements may also prove to be useful in assessing the critical population of HS-Fe centers, as the optical gap should be related to their population.

CONCLUSION

In summary, we have explored trajectories for SCO in a Fe^{2+}-based MOF, $Fe(ta)_2$, and a related Fe^{2+}-containing molecule, **Fe-ptz**. Through examination of the electron density of the ligand, as well as geometric, energetic, and electronic comparisons we have demonstrated that two competing factors determine the energetics of SCO: (i) if the ligand interacts with two or more metal centers then a perturbation to the ligand/metal interface at one end will have both a geometric and energetic impact on the metal center at the other end, and (ii) the ground-state electronic structure of Fe^{2+}-containing systems depends on the electron density of the ligand.

For systems with no long-range connectivity, spin transitions have little impact on the bulk material properties. They also have little cooperative impact on promoting subsequent transitions within the crystal. For MOFs and other extended solids, the opposite is true. As a result, this study provides a basis for the development of other framework materials with tunable SCO energetics and provides a theoretical construct in which to design ligands to promote or suppress hysteresis. Our observations highlight a potentially interesting feature in MOF ligand design. Since the maximum perturbation to a remote metal−ligand interface is achieved if the ligand linearly connects one metal center to another, one avenue for reducing the metal−metal interactions is to use ligands that orientate the metal centers such that they sit on different metal−ligand vectors. Examples include tetrabenzoic pyrene (found in NU-1000 and other MOFs)[38] and may prove to be a useful handle to tune cooperativity in SCO frameworks.

https://doi.org/10.1021/acs.jpcc.2c08816
J. Phys. Chem. C XXXX, XXX, XXX−XXX

■ ASSOCIATED CONTENT

Supporting Information

The Supporting Information is available free of charge at https://pubs.acs.org/doi/10.1021/acs.jpcc.2c08816.

DFT-optimized structure for HS-Fe-ptz (CIF)
DFT-optimized structure for HS-Fe-ta (CIF)
DFT-optimized structure for LS-Fe-ptz (CIF)
DFT-optimized structure for LS-Fe-ta (CIF)
Fe−N bond lengths, associated equilibrium structures from DFT, and additional density of states plots (PDF)

■ AUTHOR INFORMATION

Corresponding Author

Christopher H. Hendon − *Department of Chemistry and Biochemistry, University of Oregon, Eugene, Oregon 97403, United States;* orcid.org/0000-0002-7132-768X; Email: chendon@uoregon.edu

Authors

Monique C. Demuth − *Department of Chemistry and Biochemistry, University of Oregon, Eugene, Oregon 97403, United States*

Khoa N. Le − *Department of Chemistry and Biochemistry, University of Oregon, Eugene, Oregon 97403, United States*

Matthew Sciprint − *Department of Chemistry and Biochemistry, University of Oregon, Eugene, Oregon 97403, United States*

Complete contact information is available at: https://pubs.acs.org/10.1021/acs.jpcc.2c08816

Author Contributions

†M.C.D. and K.N.L. contributed equally.

Notes

The authors declare no competing financial interest.

■ ACKNOWLEDGMENTS

This material is based upon work supported by the National Science Foundation through the Division of Materials Research under Grant No. DMR-1956403. C.H.H. acknowledges the support of the Camille and Henry Dreyfus Foundation. K.N.L. is supported by the National Science Foundation Graduate Research Fellowship under Grant No. 1650114. Computations were supported by the Extreme Science and Engineering Discovery Environment (XSEDE), which is supported by National Science Foundation Grant No. ACI-1548562, and the Portland State University machine, Coeus, which is supported by the NSF (DMS1624776). We are grateful for helpful discussions with Prof. Carl K. Brozek.

■ ABBREVIATIONS

SCO, spin crossover; MOF, metal−organic framework; LS, low spin; HS, high spin; DFT, density functional theory

■ REFERENCES

(1) Gütlich, P.; Goodwin, H. A. Spin Crossover—An Overall Perspective. In *Spin Crossover in Transition Metal Compounds I*; Gütlich, P., Goodwin, H. A., Eds.; Topics in Current Chemistry; Springer: Berlin, Heidelberg, 2004; Vol. *233*, pp 1−47.

(2) Gütlich, P. Spin Crossover − Quo Vadis? *Eur. J. Inorg. Chem.* **2013**, *2013*, 581−591.

(3) Murray, K. S.; Kepert, C. J. Cooperativity in Spin Crossover Systems: Memory, Magnetism and Microporosity. In *Spin Crossover in Transition Metal Compounds I*; Gütlich, P., Goodwin, H. A., Eds.; Topics in Current Chemistry; Springer: Berlin, Heidelberg, 2004; Vol. *233*, pp 195−228.

(4) Gütlich, P.; Garcia, Y.; Goodwin, H. A. Spin Crossover Phenomena in Fe(II) Complexes. *Chem. Soc. Rev.* **2000**, *29*, 419−427.

(5) Halcrow, M. A. Structure:Function Relationships in Molecular Spin-Crossover Materials. In *Spin-Crossover Materials*; Halcrow, M. A., Ed.; John Wiley & Sons Ltd.: Oxford, UK, 2013; pp 147−169.

(6) Brooker, S. Spin Crossover with Thermal Hysteresis: Practicalities and Lessons Learnt. *Chem. Soc. Rev.* **2015**, *44*, 2880−2892.

(7) Wu, S.-G.; Wang, L.-F.; Ruan, Z.-Y.; Du, S.-N.; Gómez-Coca, S.; Ni, Z.-P.; Ruiz, E.; Chen, X.-M.; Tong, M.-L. Redox-Programmable Spin-Crossover Behaviors in a Cationic Framework. *J. Am. Chem. Soc.* **2022**, *144*, 14888−14896.

(8) Reed, D. A.; Xiao, D. J.; Gonzalez, M. I.; Darago, L. E.; Herm, Z. R.; Grandjean, F.; Long, J. R. Reversible CO Scavenging via Adsorbate-Dependent Spin State Transitions in an Iron(II)−Triazolate Metal−Organic Framework. *J. Am. Chem. Soc.* **2016**, *138*, 5594−5602.

(9) Kepenekian, M.; Le Guennic, B.; Robert, V. Primary Role of the Electrostatic Contributions in a Rational Growth of Hysteresis Loop in Spin-Crossover Fe(II) Complexes. *J. Am. Chem. Soc.* **2009**, *131*, 11498−11502.

(10) Weber, B.; Bauer, W.; Obel, J. An Iron(II) Spin-Crossover Complex with a 70 K Wide Thermal Hysteresis Loop. *Angew. Chem., Int. Ed.* **2008**, *47*, 10098−10101.

(11) Hendon, C. H.; Rieth, A. J.; Korzyński, M. D.; Dincă, M. Grand Challenges and Future Opportunities for Metal−Organic Frameworks. *ACS Cent. Sci.* **2017**, *3*, 554−563.

(12) Kurmoo, M. Magnetic Metal−Organic Frameworks. *Chem. Soc. Rev.* **2009**, *38*, 1353.

(13) Thorarinsdottir, A. E.; Harris, T. D. Metal−Organic Framework Magnets. *Chem. Rev.* **2020**, *120*, 8716−8789.

(14) Zhou, H.-C.; Long, J. R.; Yaghi, O. M. Introduction to Metal−Organic Frameworks. *Chem. Rev.* **2012**, *112*, 673−674.

(15) Mancuso, J. L.; Mroz, A. M.; Le, K. N.; Hendon, C. H. Electronic Structure Modeling of Metal−Organic Frameworks. *Chem. Rev.* **2020**, *120*, 8641−8715.

(16) Butler, K. T.; Worrall, S. D.; Molloy, C. D.; Hendon, C. H.; Attfield, M. P.; Dryfe, R. A. W.; Walsh, A. Electronic Structure Design for Nanoporous, Electrically Conductive Zeolitic Imidazolate Frameworks. *J. Mater. Chem. C* **2017**, *5*, 7726−7731.

(17) Röß-Ohlenroth, R.; Hirrle, M.; Kraft, M.; Kalytta-Mewes, A.; Jesche, A.; Krug von Nidda, H.; Volkmer, D. Synthesis, Thermal Stability and Magnetic Properties of an Interpenetrated Mn(II) Triazolate Coordination Framework. *Z. Anorg. Allg. Chem.* **2022**, *648*, e202200153.

(18) Ouellette, W.; Prosvirin, A. V.; Valeich, J.; Dunbar, K. R.; Zubieta, J. Hydrothermal Synthesis, Structural Chemistry, and Magnetic Properties of Materials of the M^{II}/Triazolate/Anion Family, Where M^{II} = Mn, Fe, and Ni. *Inorg. Chem.* **2007**, *46*, 9067−9082.

(19) Gándara, F.; Uribe-Romo, F. J.; Britt, D. K.; Furukawa, H.; Lei, L.; Cheng, R.; Duan, X.; O'Keeffe, M.; Yaghi, O. M. Porous, Conductive Metal-Triazolates and Their Structural Elucidation by the Charge-Flipping Method. *Chem.—Eur. J.* **2012**, *18*, 10595−10601.

(20) Figg, T. M.; Holland, P. L.; Cundari, T. R. Cooperativity Between Low-Valent Iron and Potassium Promoters in Dinitrogen Fixation. *Inorg. Chem.* **2012**, *51*, 7546−7550.

(21) Andreeva, A. B.; Le, K. N.; Kadota, K.; Horike, S.; Hendon, C. H.; Brozek, C. K. Cooperativity and Metal−Linker Dynamics in Spin Crossover Framework Fe(1,2,3-Triazolate)$_2$. *Chem. Mater.* **2021**, *33*, 8534−8545.

(22) Grzywa, M.; Röß-Ohlenroth, R.; Muschielok, C.; Oberhofer, H.; Błachowski, A.; Żukrowski, J.; Vieweg, D.; von Nidda, H.-A. K.; Volkmer, D. Cooperative Large-Hysteresis Spin-Crossover Transition in the Iron(II) Triazolate [Fe(ta)$_2$] Metal−Organic Framework. *Inorg. Chem.* **2020**, *59*, 10501−10511.

(23) García-López, V.; Palacios-Corella, M.; Cardona-Serra, S.; Clemente-León, M.; Coronado, E. Spin-Crossover Iron(II) Complex Showing Thermal Hysteresis around Room Temperature with Symmetry Breaking and an Unusually High T (LIESST) of 120 K. *Chem. Commun.* **2019**, *55*, 12227−12230.
(24) Zheng, C.; Jia, S.; Dong, Y.; Xu, J.; Sui, H.; Wang, F.; Li, D. Symmetry Breaking and Two-Step Spin-Crossover Behavior in Two Cyano-Bridged Mixed-Valence $\{Fe^{III}_2(\mu\text{-}CN)_4Fe^{II}_2\}$ Clusters. *Inorg. Chem.* **2019**, *58*, 14316−14324.
(25) Shatruk, M.; Phan, H.; Chrisostomo, B. A.; Suleimenova, A. Symmetry-Breaking Structural Phase Transitions in Spin Crossover Complexes. *Coord. Chem. Rev.* **2015**, *289-290*, 62−73.
(26) Vela, S.; Paulsen, H. Cooperativity in Spin Crossover Systems. An Atomistic Perspective on the Devil's Staircase. *Inorg. Chem.* **2018**, *57*, 9478−9488.
(27) Park, J. G.; Aubrey, M. L.; Oktawiec, J.; Chakarawet, K.; Darago, L. E.; Grandjean, F.; Long, G. J.; Long, J. R. Charge Delocalization and Bulk Electronic Conductivity in the Mixed-Valence Metal−Organic Framework $Fe(1,2,3\text{-Triazolate})_2(BF_4)_x$. *J. Am. Chem. Soc.* **2018**, *140*, 8526−8534.
(28) Sun, L.; Hendon, C. H.; Park, S. S.; Tulchinsky, Y.; Wan, R.; Wang, F.; Walsh, A.; Dincă, M. Is Iron Unique in Promoting Electrical Conductivity in MOFs? *Chem. Sci.* **2017**, *8*, 4450−4457.
(29) Muschielok, C.; Reiner, A.; Röß-Ohlenroth, R.; Kalytta-Mewes, A.; Volkmer, D.; Wixforth, A.; Oberhofer, H. Combining Theory and Experiments To Study the Influence of Gas Sorption on the Conductivity Properties of Metal−Organic Frameworks. *ACS Appl. Mater. Interfaces* **2022**, *14*, 33662−33674.
(30) Hauser, A. Intersystem Crossing in the $[Fe(Ptz)_6](BF_4)_2$ Spin Crossover System (Ptz = 1-propyltetrazole). *J. Chem. Phys.* **1991**, *94*, 2741−2748.
(31) Kresse, G.; Furthmüller, J. Efficiency of Ab-Initio Total Energy Calculations for Metals and Semiconductors Using a Plane-Wave Basis Set. *Comput. Mater. Sci.* **1996**, *6*, 15−50.
(32) Kresse, G.; Furthmüller, J. Efficient Iterative Schemes for *ab initio* Total-Energy Calculations Using a Plane-Wave Basis Set. *Phys. Rev. B* **1996**, *54*, 11169−11186.
(33) Ernzerhof, M.; Perdew, J. P. Generalized Gradient Approximation to the Angle- and System-Averaged Exchange Hole. *J. Chem. Phys.* **1998**, *109*, 3313−3320.
(34) Janesko, B. G.; Henderson, T. M.; Scuseria, G. E. Screened Hybrid Density Functionals for Solid-State Chemistry and Physics. *Phys. Chem. Chem. Phys.* **2009**, *11*, 443−454.
(35) Schimka, L.; Harl, J.; Kresse, G. Improved Hybrid Functional for Solids: The HSEsol Functional. *J. Chem. Phys.* **2011**, *134*, 024116.
(36) : Frisch, M. J.; Trucks, G. W.; Schlegel, H. B.; Scuseria, G. E.; Robb, M. A.; Cheeseman, J. R.; Scalmani, G.; Barone, V.; Petersson, G. A.; H. Nakatsuji, X., et al. *Gaussian 09, Revision E.01*; Gaussian, Inc., Wallingford, CT, 2016.
(37) Binning, R. C.; Curtiss, L. A. Compact Contracted Basis Sets for Third-Row Atoms: Ga-Kr. *J. Comput. Chem.* **1990**, *11*, 1206−1216.
(38) Mondloch, J. E.; Bury, W.; Fairen-Jimenez, D.; Kwon, S.; DeMarco, E. J.; Weston, M. H.; Sarjeant, A. A.; Nguyen, S. T.; Stair, P. C.; Snurr, R. Q.; Farha, O. K.; Hupp, J. T. Vapor-Phase Metalation by Atomic Layer Deposition in a Metal−Organic Framework. *J. Am. Chem. Soc.* **2013**, *135*, 10294−10297.

https://doi.org/10.1021/acs.jpcc.2c08816
J. Phys. Chem. C XXXX, XXX, XXX−XXX